SAC phosphoinositide phosphatases at the tonoplast mediate vacuolar function in *Arabidopsis*

Petra Nováková[a,b,c], Sibylle Hirsch[b,c,1], Elena Feraru[b,c,2], Ricardo Tejos[b,c,3], Ringo van Wijk[d], Tom Viaene[b,c], Mareike Heilmann[e], Jennifer Lerche[e], Riet De Rycke[b,c], Mugurel I. Feraru[b,c,2], Peter Grones[a,b,c], Marc Van Montagu[b,c,4], Ingo Heilmann[e], Teun Munnik[d], and Jiří Friml[a,b,c,4]

[a]Institute of Science and Technology Austria, 3400 Klosterneuburg, Austria; [b]Department of Plant Systems Biology, Flanders Institute for Biotechnology and [c]Department of Plant Biotechnology and Bioinformatics, Ghent University, 9052 Ghent, Belgium; [d]Section of Plant Physiology, Swammerdam Institute for Life Sciences, University of Amsterdam, 1090 GE, Amsterdam, The Netherlands; and [e]Department of Cellular Biochemistry, Institute for Biochemistry and Biotechnology, Martin-Luther-University Halle-Wittenberg, 06099 Halle, Germany

Contributed by Marc Van Montagu, January 2, 2014 (sent for review December 4, 2013)

Phosphatidylinositol (PtdIns) is a structural phospholipid that can be phosphorylated into various lipid signaling molecules, designated polyphosphoinositides (PPIs). The reversible phosphorylation of PPIs on the 3, 4, or 5 position of inositol is performed by a set of organelle-specific kinases and phosphatases, and the characteristic head groups make these molecules ideal for regulating biological processes in time and space. In yeast and mammals, PtdIns3P and PtdIns(3,5)P_2 play crucial roles in trafficking toward the lytic compartments, whereas the role in plants is not yet fully understood. Here we identified the role of a land plant-specific subgroup of PPI phosphatases, the suppressor of actin 2 (SAC2) to SAC5, during vacuolar trafficking and morphogenesis in *Arabidopsis thaliana*. SAC2–SAC5 localize to the tonoplast along with PtdIns3P, the presumable product of their activity. In SAC gain- and loss-of-function mutants, the levels of PtdIns monophosphates and bisphosphates were changed, with opposite effects on the morphology of storage and lytic vacuoles, and the trafficking toward the vacuoles was defective. Moreover, multiple *sac* knockout mutants had an increased number of smaller storage and lytic vacuoles, whereas extralarge vacuoles were observed in the overexpression lines, correlating with various growth and developmental defects. The fragmented vacuolar phenotype of *sac* mutants could be mimicked by treating wild-type seedlings with PtdIns(3,5)P_2, corroborating that this PPI is important for vacuole morphology. Taken together, these results provide evidence that PPIs, together with their metabolic enzymes SAC2–SAC5, are crucial for vacuolar trafficking and for vacuolar morphology and function in plants.

membrane lipids | epidermal cells | membrane fusion and fission

Polyphosphoinositides (PPIs) are a class of signaling membrane lipids, comprising the phosphorylated products of phosphatidylinositol (PtdIns). PPIs perform a dual function as scaffolding signals and precursors for other molecular messengers, which, together with their specific distribution at different intracellular membranes, makes PPIs important mediators of a wide variety of cellular processes, such as membrane trafficking and homeostasis, cytoskeleton organization, nuclear signaling, and stress responses (1–5). The metabolism of PPIs is regulated by specific kinases, phosphatases, and phospholipases to tightly control the concentration and intracellular localization of different lipid pools (2, 6, 7).

In yeast, two phosphoinositide (PI) types, PtdIns3P and PtdIns(3,5)P_2, and their interconversion have been shown to play crucial roles in trafficking toward the vacuole, regulation of vacuolar pH, and vacuolar membrane fusion and fission (8–11). In yeast and mammals, production and degradation of PtdIns(3,5)P_2 involve the PtdIns3P 5-kinase Fab1p/PIKfyve and the antagonistic phosphatase factor-induced gene/suppressor of actin 3 (Fig4/Sac3), respectively (8, 12–14). Impairment of genes implicated in PtdIns(3,5)P_2 metabolism has deleterious consequences in yeast, plants, and mammals (8, 15–19), demonstrating an essential function of this minor phospholipid. Recent observations also hint at a role for PPIs in plant vacuoles (18–20), but the data are scarce and remain inconclusive.

Advances in deciphering various cellular roles of PIs include insights into the phosphatases responsible for hydrolyzing PPIs. A group of phosphatases, designated suppressor of actin (SAC) domain phosphatases, has been identified in lower eukaryotes, mammals, and plants (21). Whereas yeast and humans have only five genes harboring the SAC domain, the genome of the model plant *Arabidopsis thaliana* contains nine genes, of which some have been functionally characterized and demonstrated to be involved in the regulation of stress responses (22–24), polarized root hair expansion (3), or cell wall formation (25).

Here we show that the functionally uncharacterized group of *Arabidopsis* SAC2–SAC5 proteins that is orthologous to the yeast Fig4p is involved in PPI metabolism. SAC2–SAC5 localize along

Significance

Polyphosphoinositides (PPIs) are derivatives of the membrane lipid phosphatidylinositol that occur in minor amounts in eukaryotic membranes. PPIs have regulatory effects on various cellular processes, but their roles in plants are currently not well-understood. Plant growth relies largely on turgor-driven cell expansion, which at the subcellular level is linked to vacuolar dynamics. We identified an unknown subgroup of tonoplast-associated enzymes from *Arabidopsis thaliana*, the suppressor of actin 2 (SAC2) to SAC5, that modify PPI levels in plants and influence vacuolar morphology. *Arabidopsis* lines overexpressing or deficient in SAC isoforms display growth aberrations consistent with defective vacuolar function and turgor control. The data hint at PPI-regulated processes in the plant tonoplast and link PPIs to the control of turgor-driven cell expansion and, possibly, other vacuolar functions.

Author contributions: P.N., S.H., E.F., R.T., M.V.M., I.H., T.M., and J.F. designed research; P.N., S.H., E.F., R.T., R.v.W., T.V., M.H., J.L., R.D.R., M.I.F., and P.G. performed research; P.N., S.H., E.F., R.T., R.v.W., M.H., I.H., T.M., and J.F. analyzed data; and P.N., S.H., R.T., T.V., I.H., T.M., and J.F. wrote the paper.

The authors declare no conflict of interest.

Data deposition: The sequences reported in this paper have been deposited in the GenBank database [accession nos. AAP49834.1 (At1G22620, SAC1), AAP49835.1 (At3G14205, SAC2), AAP49836.1 (At3G43220, SAC3), AAP49837.1 (At5G20840, SAC4), AAP49838.1 (At1G17340, SAC5), and AAC49823.1 (At5G46860, SYP22)].

[1]Present address: Institute of Plant Biology, University of Zürich, CH-8008 Zürich, Switzerland.

[2]Present address: Department of Applied Genetics and Cell Biology, University of Natural Resources and Life Sciences (BOKU), 1190 Vienna, Austria.

[3]Present address: Plant Molecular Biology Laboratory, Department of Biology, Faculty of Sciences, University of Chile, Santiago 7800003, Chile.

[4]To whom correspondence may be addressed. E-mail: marc.vanmontagu@ugent.be or jiri.friml@ist.ac.at.

This article contains supporting information online at www.pnas.org/lookup/suppl/doi:10.1073/pnas.1324264111/-/DCSupplemental.

with PtdIns3P to the tonoplast and maintain the morphology of storage and lytic vacuoles. Our results demonstrate the crucial role of PPIs and SAC domain phosphatases in the function and morphology of vacuoles in plants.

Results and Discussion

Evolution of SAC Phosphatases in the Green Lineage. We reconstructed the evolution of SAC domain-containing proteins in the green lineage (Fig. S1) based on full-length protein sequences. Similar to previous reports (26), we identified three major clades containing fungal, algal, and land plant sequences that probably originated before or early during eukaryote diversification. The first clade contains *Arabidopsis* SAC1–SAC5, which is most homologous to the yeast Fig4p protein, but with SAC1 distinct from the SAC2–SAC5 subgroup that probably originated after land plant diversification and, subsequently, led to multiple copies in *Arabidopsis*. The second clade consists of SAC6–SAC8, homologous to the yeast Sac1p protein that plays a role in the maintenance of PtdIns4P levels and to the inositol polyphosphate 5-phosphatases INP51–INP53 that are also known as the synaptojanin-like proteins SJL1, SJL2, and SJL3 (27, 28). The third clade contains SAC9, the longest of the SAC domain-containing proteins from *Arabidopsis*, but with no yeast homolog, although homologs can be identified in other fungal species. We focused on the first clade, particularly on the functionally uncharacterized SAC2–SAC5 subgroup that diverged in land plants and is seemingly distinct from the previously characterized SAC1 (25).

SAC2–SAC5 Phosphatases Localize to the Tonoplast. The closest ortholog of SAC1–SAC5 in yeast is Fig4p, which exhibits a phosphatase activity against PtdIns(3,5)P_2 and is localized to the tonoplast of the central vacuole (12, 13). In vitro, *Arabidopsis* SAC1 also exhibits phosphatase activity toward PtdIns(3,5)P_2, but localizes to the Golgi apparatus (25). To gain insights into the subcellular localization of SAC2–SAC5, we generated transgenic *Arabidopsis* lines expressing *SAC* genes fused to green fluorescent protein (GFP) or red fluorescent protein (RFP) under their native or 35S constitutive promoters. In root epidermal cells of plants expressing *35S::SAC2-GFP* to *35S::SAC5-GFP*, the fluorescent signal was detected mostly at the tonoplast, with faint fluorescence in the cytoplasm (Fig. 1*A* and Fig. S2 *A–C*). *SAC2-GFP* and *SAC5-GFP* expression under the endogenous promoters localized only in the tonoplast (Fig. 1 *B* and *C*). To confirm the tonoplast localization, we used *SAC5* as a representative and performed colocalizations with various subcellular markers. *35S::SAC5-RFP* colocalized with syntaxin SYP22-yellow fluorescent protein (YFP), which is predominantly localized to the vacuolar membrane and weakly localized to the prevacuolar compartments (PVCs) (29) (Fig. 1*D* and Fig. S2 *D–F*). The endocytic tracer *N*-(3-triethylammoniumpropyl)-4-(6-[4-(diethylamino) phenyl]hexatrienyl) pyridinium dibromide (FM4-64) (8 μM), which after a prolonged treatment labels the vacuolar membrane (30, 31), colocalized with *SAC5::SAC5-GFP* (Fig. 1*E* and Fig. S2 *G–I*), and LysoTracker Red, which labels acidic compartments (32, 33), is surrounded by the fluorescent signal of *SAC5::SAC5-GFP* (Fig. 1*F* and Fig. S2 *J–L*). In contrast, immunolocalization of markers for the Golgi apparatus (SEC21), *trans*-Golgi network (ARF1), and PVC (ARA7/RHA1) did not show any colocalization with *35S::SAC5-GFP* (Fig. S2 *M–U*). Together, these results show that SAC2–SAC5 localize to the tonoplast.

Gain-of-Function Phenotypes of SAC Phosphatases. To investigate SAC1–SAC5 function in *Arabidopsis*, we generated and analyzed the phenotype of the overexpression lines. We found that *35S::SAC1-GFP* (Fig. S3*B*) had longer roots (Fig. S3*D*), longer hypocotyls (Fig. S3*F*), and an increased number of lateral roots compared with control seedlings (Fig. S3*H*). In contrast, seedlings overexpressing *SAC2-GFP* to *SAC5-GFP* showed variable phenotypes; several lines were strongly defective in growth and were not viable after transfer to soil (Fig. 2 *A* and *B*), whereas seedlings with a weaker *SAC2–SAC5* expression (Fig. S3*A*) showed milder phenotypes, including epinastic leaves (Fig. 2 *C* and *D* and Fig. S4 *A–D*), enhanced lateral root formation (Fig. 2 *F*, *G*, and *M*), and shorter hypocotyls (Fig. 2 *H–M*). In addition, the percentage of arrested or agravitropic seedlings was higher when grown on medium without sucrose (Fig. 2*E*). These results show that SAC2–SAC5 display similar gain-of-function phenotypes that are indicative of the important roles of these phosphatases for plant growth.

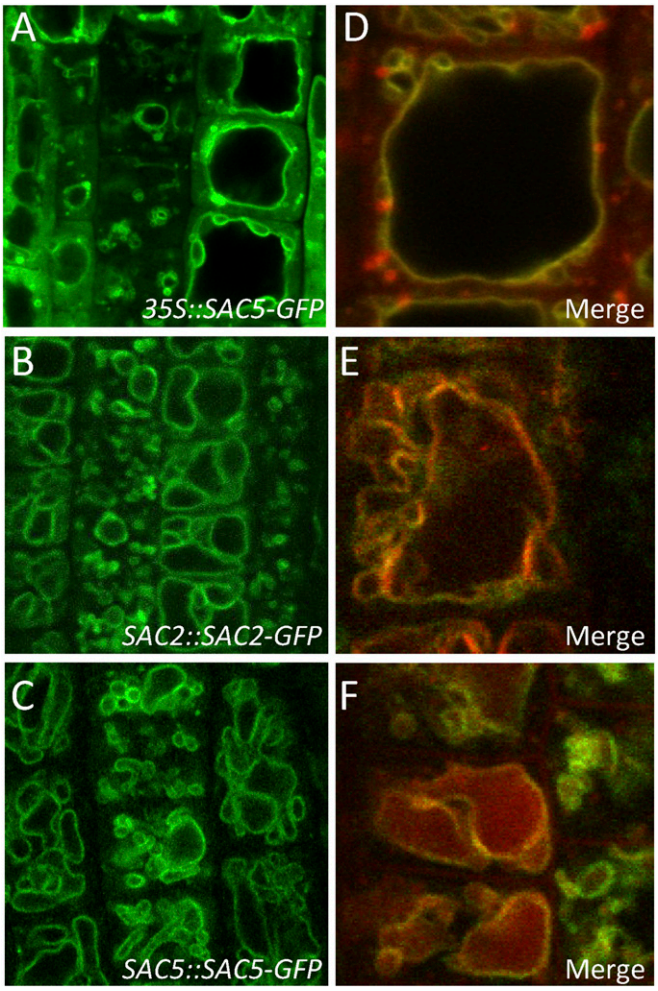

Fig. 1. Localization of SAC2–SAC5 to the tonoplast. (*A–C*) Fluorescence microscopy of SAC2-GFP and SAC5-GFP, which localize to the tonoplast under the 35S (*A*) and native promoters (*B* and *C*). (*D–F*) Colocalization of SYP22-YFP with *35S::SAC5-RFP* (*D*) and *SAC5::SAC5-GFP* with the endocytic tracer FM4-64 (8 μM; 3.5 h) (*E*) or LysoTracker Red (2 μM; 1 h) (*F*), which label acidic compartments.

Loss-of-Function Phenotypes of SAC Phosphatases. To dissect the function of SAC phosphatases in *Arabidopsis*, we isolated T-DNA insertional lines for *SAC1–SAC5* (Fig. S4*E*) and characterized the expression levels for the disrupted alleles (Fig. S4*F*). It has been reported previously that the *fra7* allele of *SAC1* causes a truncation of the C terminus of the SAC1 protein, resulting in altered subcellular localization and shorter roots and hypocotyls (25). We analyzed true *sac1* knockout mutants and found that they displayed longer roots, shorter hypocotyls, and an increased lateral root formation (Fig. S3 *C*, *E*, and *G*). In contrast, single knockout mutants of *sac3*, *sac4*, and *sac5* and the knockdown *sac2* mutant had very weak or no phenotypic defects.

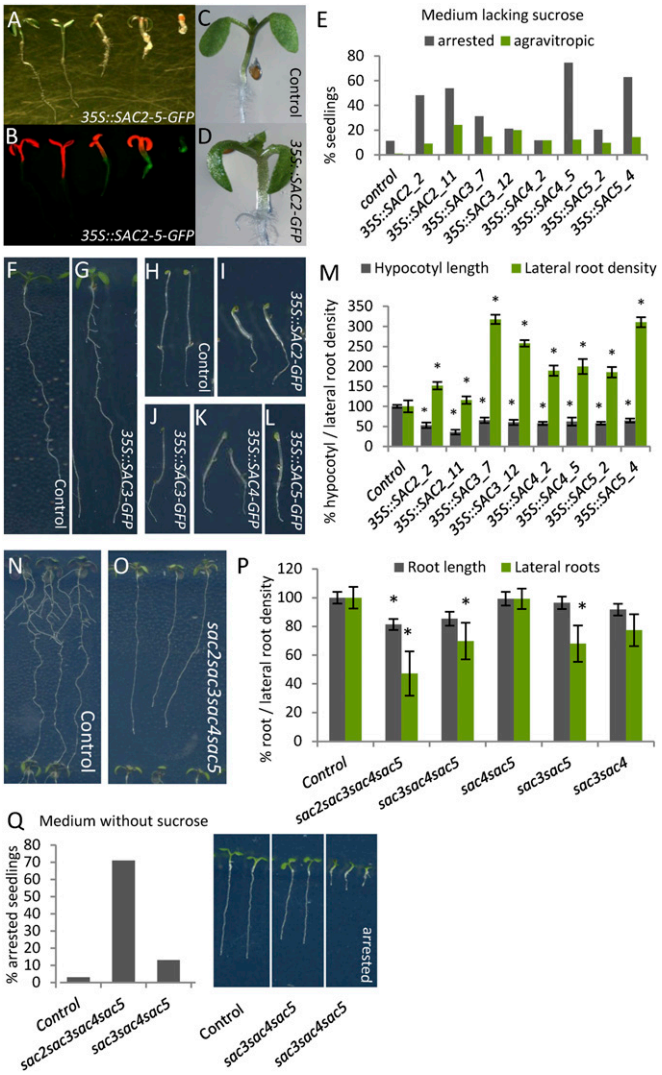

Fig. 2. Gain-of-function and loss-of-function phenotypes of SAC phosphatases. (*A* and *B*) Inhibited growth by strong expression of *35S::SAC2-GFP* to *35S::SAC5-GFP*. Pictures were taken under the microscope with transmitted (*A*) and fluorescent light (*B*). Green and red represent the GFP fluorescence and autofluorescence of green tissue, respectively. (*C* and *D*) Epinastic leaves in *35::SAC2-GFP* (*D*) compared with the control (*C*). (*E*) Higher number of arrested and agravitropic 7-d-old seedlings grown on medium without sucrose than that of control seedlings grown under the same conditions (n = 50–70 roots per experiment). (*F*, *G*, and *M*) Ten-day-old seedlings of *35S::SAC2-GFP* to *35S::SAC5-GFP* showing an increased lateral root formation compared with the control (n = 20 roots per experiment). (*H*–*M*) Dark-grown 5-d-old seedlings of *35::SAC2-GFP* to *35S::SAC5-GFP* with a reduced hypocotyl length (n = 20–25 hypocotyls per experiment). (*N*–*P*) Twelve-day-old seedlings of multiple *sac* mutants with a reduced lateral root formation compared with the control (n = 15 roots per experiment). (*P*) Seven-day-old seedlings of triple and quadruple *sac* mutants show reduced root growth compared with the control (n = 30 roots per experiment). (*Q*) Seven-day-old triple and quadruple *sac* mutants displaying an increased number of arrested seedlings on medium without sucrose compared with the control grown under the same conditions (n = 70–90 roots per experiment). Error bars represent SE. *t* test, $*P < 0.001$.

To assess possible genetic redundancies, we generated double, triple, and quadruple mutants. Although double mutants did not show clear phenotypic differences compared with wild-type controls, seedlings of the *sac2 sac3 sac4 sac5* quadruple mutant and *sac3 sac4 sac5* triple mutant showed shorter roots, a decreased number of lateral roots (Fig. 2 *N*–*P*), and an increased number of arrested seedlings when grown on medium lacking sucrose (Fig. 2*Q*). These results, together with the gain-of-function phenotypes, show that SAC2–SAC5 have essential and redundant functions for plant growth that are distinct from those of SAC1.

SAC Phosphatases Mediate Vacuolar Morphology. Some aspects of plant growth that are altered in *sac* knockout and overexpression lines are turgor-driven and depend on vacuolar function. Given the localization of SAC2–SAC5 at the tonoplast, we analyzed the vacuolar morphology in roots of *sac* knockout and overexpression lines. Labeling of the *sac3 sac4 sac5* triple knockout mutant with FM4-64 for 3.5 h and the *sac2 sac3 sac4 sac5* quadruple mutant with LysoTracker Red and the localization of the tonoplast/PVC marker SYP22-YFP revealed a seemingly more fragmented vacuole in the mutant than in control seedlings (Fig. 3 *A*–*D* and Fig. S5 *A* and *B*). Closer investigation revealed that the vacuolar phenotype of the *sac2 sac3 sac4 sac5* quadruple mutant varied, but that in ∼50–60% of the roots the vacuoles were clearly more fragmented. We also analyzed the ultrastructure of root cells of the *sac3 sac4* and *sac3 sac4 sac5* mutants by transmission electron microscopy (TEM). In accordance with the results from the fluorescence microscopy, abnormal vacuole numbers and sizes were observed by TEM (Fig. 3 *E*–*G*). In contrast to the loss-of-function mutants, the overexpression of SAC phosphatases resulted in larger vacuoles than those of controls (Fig. 3 *H* and *I* and Fig. S5 *C* and *D*).

Both SAC gain-of-function and loss-of-function mutants displayed arrested growth on medium without sucrose, which is typical for mutants defective in protein storage vacuoles (PSVs) (33–36). Therefore, we investigated whether the SAC phosphatases affected the PSV morphology in seeds where it can be easily visualized by autofluorescence. The *sac2 sac3 sac4 sac5* quadruple mutant had an increased number of smaller PSVs in contrast to the overexpression lines, with usually one enlarged PSV surrounded by smaller vacuoles (Fig. 3 *J*–*L*). Overall, these analyses revealed that *sac* loss-of-function mutants have fragmented storage and lytic vacuoles, whereas gain-of-function mutants contain large vacuoles. Hence, SAC2–SAC5 phosphatases might be redundant for the maintenance of the vacuolar morphology.

Role of SAC Phosphatases in Trafficking Toward the Vacuole. To test whether the SAC-related vacuolar defects were accompanied by defects in the trafficking route toward the vacuole, we used wortmannin, an inhibitor of PtdIns kinase activities in plants that causes a dilatation/swelling of the PVCs (37, 38). Localization of the vacuolar and PVC marker SYP22-YFP revealed more, and less dilated, compartments in the *sac3 sac4 sac5* triple mutant after treatment with 33 μM wortmannin compared with the control. In contrast, the *SAC5-GFP* overexpression line displayed less and enlarged wortmannin-sensitive compartments (Fig. 4 *A*–*F*). To analyze protein trafficking in *sac* mutants, we used the fungal toxin Brefeldin A (BFA) that interferes with various vesicle-trafficking processes, including recycling to the plasma membrane and vacuolar trafficking (35, 39, 40). Specifically, we examined the endocytic and vacuolar trafficking of the auxin transporter PIN-FORMED2 (PIN2) (41), which is a plasma membrane protein with a well-established trafficking route to the vacuole for degradation (35, 42, 43). Treatment with 50 μM BFA for 90 min in both the triple mutant *sac3 sac4 sac5* and the *35S::SAC5-GFP* line revealed a higher increased number of BFA-induced PIN2-containing aggregations per cell than that in the control (Fig. 4 *G*–*J*). The BFA bodies were clearly smaller in size in the overexpression line. Taken together, the effects of wortmannin and BFA on vacuolar trafficking suggest that SAC phosphatases are required not only for morphology and maintenance of vacuoles but also for the regulation of protein trafficking toward the vacuole.

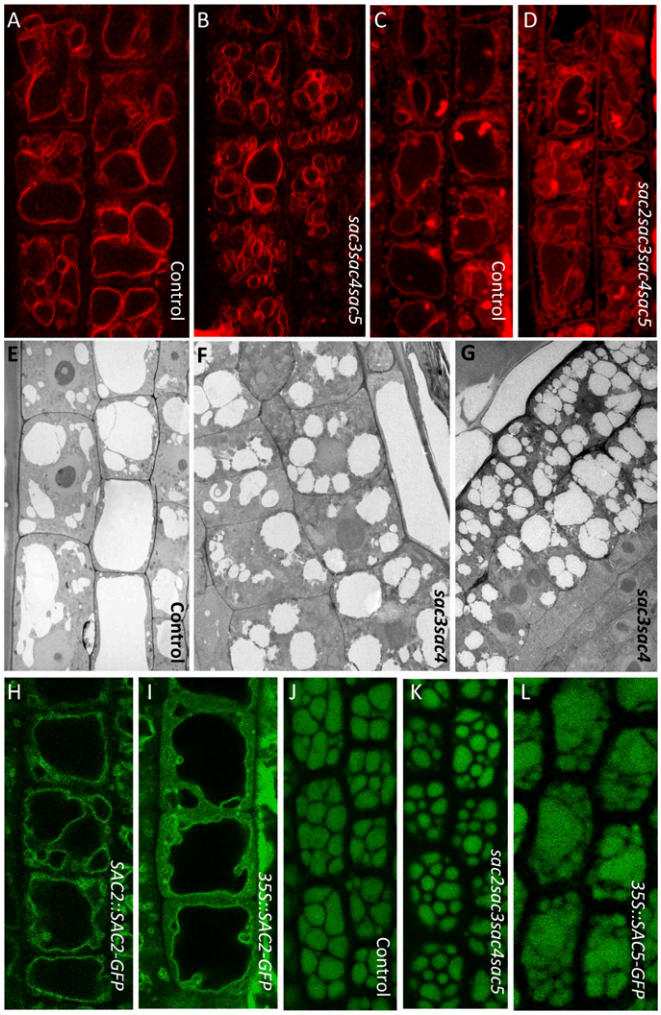

Fig. 3. Aberrant vacuolar morphology in *sac* mutants. (*A* and *B*) Epidermal cells of control (*A*) and *sac3 sac4 sac5* mutant (*B*) stained with FM4-64 (8 μM) showing an increased vacuolar fragmentation in the mutant. (*C* and *D*) Epidermal cells of control (*C*) and *sac2 sac3 sac4 sac5* mutant (*D*) stained with LysoTracker Red (2 μM) showing an increased number of vacuoles in the mutant. (*E*–*G*) Electron micrographs of the vacuolar morphology in the control (*E*) and *sac3 sac4* mutant (*F* and *G*). (*H* and *I*) Mainly one enlarged vacuole per cell in the epidermal cells of the overexpressing lines *35S::SAC2-GFP* (*I*) versus *SAC2::SAC2-GFP* control (*H*). (*J*–*L*) Increased number of smaller protein storage vacuoles of embryonic root cells of *sac2 sac3 sac4 sac5* mutants (*K*), in contrast to *35S::SAC5-GFP*, with enlarged PSVs (*L*) compared with the control (*J*).

PPIs Play a Role in Vacuoles of *Arabidopsis*. The $PtdInsP_2$ levels of the different SAC phosphatase plants were analyzed with a combination of TLC and gas chromatography (44). In contrast to all previous reports that use this method, the attempt to distinguish the $PtdInsP_2$ isomers relevant for this study, $PtdIns(3,5)P_2$ and $PtdIns(4,5)P_2$, was a substantial analytical challenge because of their extremely low quantities. Generally, the overexpression lines for *SAC2–SAC5* seemed to display reduced levels of $PtdIns(3,5)P_2$ (Fig. 5*A*), consistent with the predicted role in the hydrolysis of this lipid. The patterns observed were not statistically significant when a 95% confidence interval was used, but were consistently observed in three independent biological experiments, each representing three to six individual pools of plants. Because the analysis of nonlabeled $PtdIns(3,5)P_2$ and $PtdIns(4,5)P_2$ pushed the detection limits, the data had inherently high errors and must be interpreted with caution. Surprisingly, with the exception of the SAC5 overexpressor, the levels of $PtdIns(4,5)P_2$ were high in the SAC overexpression lines (Fig. 5*B*), possibly indicating a compensatory reaction. Such compensatory transcript increases of phosphoinositide kinases upon deletion of isoenzymes have been observed previously (45).

A compensatory reaction is also supported by the increased incorporation of $[^{32}P]P_i$ radiolabel into $PtdIns(4,5)P_2$ in seedlings of the overexpressor lines (Fig. 5*C*). Furthermore, the *sac3 sac4 sac5* triple mutant also displayed increased $PtdIns(4,5)P_2$, whereas $PtdIns(3,5)P_2$ changed to a much lesser degree (Fig. 5 *A* and *B*). The overall patterns indicate a thus far unknown interplay between enzymes forming $PtdIns(3,5)P_2$ and $PtdIns(4,5)P_2$ that will require more detailed scrutiny in the future. The interpretation of the overexpression of individual SAC isoforms is the easiest, because the perturbations target defined individual genes. The observed reduction in $PtdIns(3,5)P_2$ upon overexpression of *SAC2–SAC5* (Fig. 5*A*) is consistent with the related yeast Fig4p, hydrolyzing $PtdIns(3,5)P_2$ (12). The results from the analysis of the *sac3 sac4 sac5* triple mutant are harder to explain, because more than one enzyme is targeted, possibly resulting in a more complex metabolic adaptation. The observation that the levels of $PtdIns(3,5)P_2$ were not altered in the triple mutant, whereas that of $PtdIns(4,5)P_2$ was increased (Fig. 5*A*), suggests a compensatory response and a possible link between the two $PtdInsP_2$ isomers that had not been reported previously. The subcellular distribution of lipids might be the reason for the observed patterns, but at this point there is no reporter that indicates the $PtdIns(3,5)P_2$ distribution. Assuming that $PtdIns(3,5)P_2$ resides mainly in the tonoplast, as suggested by the previously reported effect of Fab1-like phosphoinositide kinases on vacuolar function (19), it might be required to relate the levels of $PtdIns(3,5)P_2$ to the tonoplast surface area rather than the fresh weight as a reference. Moreover, as the *sac* mutants displayed fragmented vacuoles and, thus, an enhanced tonoplast area, the amount of $PtdIns(3,5)P_2$ per tonoplast area might actually be much lower in the triple mutant than that in the controls. Reciprocally, $PtdIns(3,5)P_2$ levels might be higher for *SAC*

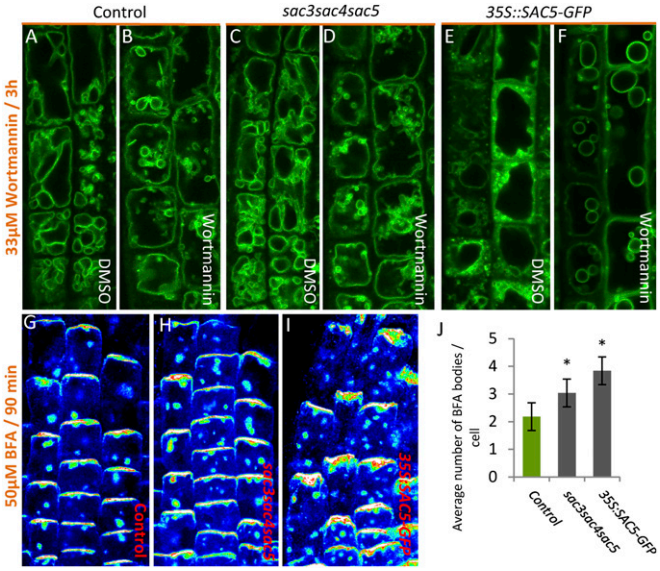

Fig. 4. Defective vacuolar trafficking in *sac* mutants. (*A*–*F*) SYP22-YFP vacuolar morphology in the control (*A*) and *sac* mutants (*C* and *E*) treated with dimethylsulfoxide and in the control (*B*) and *sac* mutants (*D* and *F*) treated with 33 μM wortmannin for 3 h. (*G*–*J*) Immunolocalization of anti-PIN2 after treatment with 50 μM BFA for 1.5 h in control (*G*) and *sac* mutants (*H* and *I*). (*J*) The average number of BFA bodies is quantified as the number of BFA bodies observed in the maximal projection of confocal images. Error bars represent SD. $*P < 0.001$, *t* test.

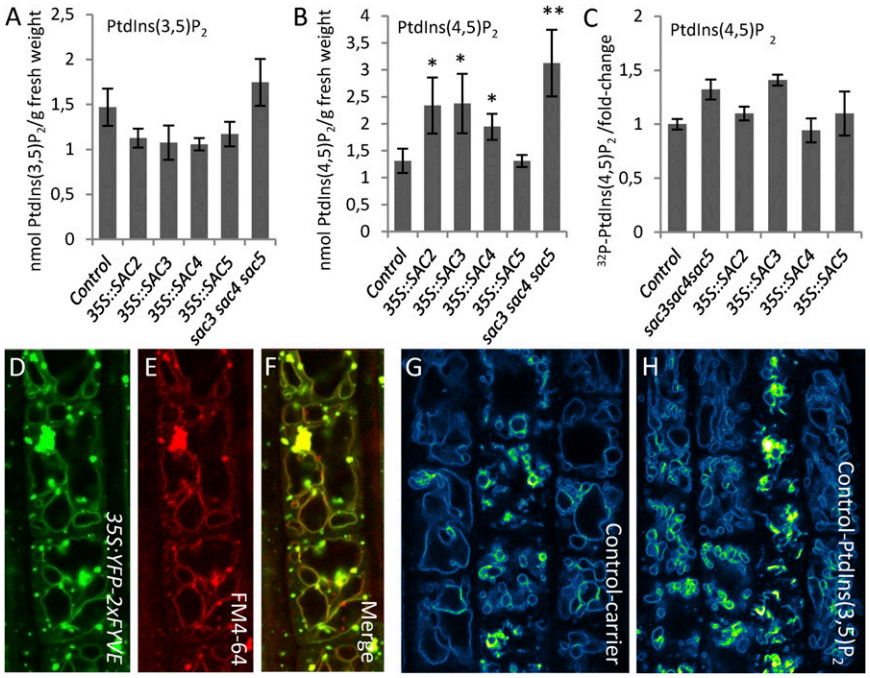

Fig. 5. PIP2 effect on vacuolar morphology. (*A*) Mass levels of PtdIns(3,5)P_2 in roots of 2-wk-old plants of overexpression or knockout lines of SAC phosphatases (*sac3 sac4 sac5*, $P = 0.218$; *35S::SAC2*, $P = 0.134$; *35S::SAC3*, $P = 0.101$; *35S::SAC4*, $P = 0.051$; *35S::SAC5*, $P = 0.190$). (*B*) Mass levels of PtdIns(4,5)P_2 in roots of 2-wk-old plants of overexpression or knockout lines of SAC phosphatases (*sac3 sac4 sac5*, $P = 0.007$; *35S::SAC2*, $P = 0.039$; *35S::SAC3*, $P = 0.049$; *35S::SAC4*; $P = 0.044$; *35S::SAC5*, $P = 0.500$). (*C*) [^{32}P] PtdInsP_2 levels in overnight $^{32}P_i$-labeled 6-d-old seedlings of wild type, triple mutant, or overexpressors. (*D–F*) PI3P-specific biosensor *35S::YFP-2xFYVE* (*D*) colocalized with the endocytic tracer FM4-64 that stained the tonoplast and PVC (8 μM; 3 h) (*E* and *F*). (*G* and *H*) Vacuole morphology of nontreated control (*G*) versus control treated with 1 μM PtdIns(3,5)P_2 (*H*). Error bars represent SD (*A* and *B*) and SE (*C*). $*P < 0.05$, $**P < 0.01$, *t* test.

overexpressors that showed an increased coalescence of vacuoles and a reduced tonoplast area. The PtdInsP_2 levels associated with the tonoplast are possibly maintained at a somewhat constant level. A compensatory increase in PtdInsP_2 levels may additionally hint at a need for the presence of anionic lipids in vacuolar function. There is emerging evidence that PPIs play a conserved role in plant vacuoles (18–20, 46), as strongly supported by our data on the presence of SAC phosphatases in the tonoplast (Fig. 1) and, in part, by the lipid analyses. To test this hypothesis, we analyzed the subcellular distribution of PtdIns3P, the putative product of SAC1–SAC5 activity. We used the fluorescent YFP-2xFYVE biosensor that specifically binds to PtdIns3P via its FYVE domain (20, 46). Analysis of the *35S::YFP-2xFYVE* transgenic lines revealed YFP-2xFYVE localization on the late endosomes/PVC and also prominently in the tonoplast (Fig. 5*D*), as confirmed by colocalization with the endocytic tracer FM4-64 (Fig. 5 *E* and *F*). Furthermore, we were able to mimic the fragmented vacuole phenotype of *sac* loss-of-function mutants (Fig. 3) by treating wild-type seedlings with 1 μM PtdIns(3,5)P_2 (Fig. 5 *G* and *H*), confirming that PIs are important for vacuolar morphology in plants.

Conclusion

PPI isomers and their differential subcellular localization are important factors for multiple cellular processes, including function of lytic organelles, such as vacuoles and lysosomes in yeast and mammals (3, 11, 47), but it is still unclear whether a similar function is conserved in plants. Here we provide conclusive insights into the role of PPIs in plant vacuolar function by functional analysis of SAC2–SAC5, a previously uncharacterized subgroup of PPI phosphatases in *Arabidopsis* that is specific for land plants. Together with SAC1, SAC2–SAC5 are orthologs of the yeast Fig4p phosphatase that plays a dual role in the synthesis and turnover of PtdIns(3,5)P_2 by acting in a vacuole-associated complex with FAB1p kinase and the adaptor proteins Vac7p and Vac14p (12, 13, 48). Homologs of these members of this yeast protein complex have been identified in the *Arabidopsis* genome, except for Vac7 (49); however, they do not localize at the tonoplast, as illustrated by the AtFAB1 kinase at the endosomes (50) and SAC1 at the Golgi apparatus (25). Thus, the mechanisms for synthesis and turnover of PtdIns(3,5)P_2 in *Arabidopsis* differ seemingly from those in yeast.

In contrast, our experiments demonstrate that SAC2–SAC5 localize to the tonoplast, as observed for Fig4p and its vacuolar complex in yeast. Analysis of loss- and gain-of-function lines has revealed that these genes are redundantly required for multiple aspects of growth and development. Some of the phenotypic characteristics of the mutants, such as decreased viability on medium without sugar, are reminiscent of mutants defective in function and trafficking to the vacuoles (33–36). Cell biological analysis revealed that elevated SAC2–SAC5 expression leads to larger and less numerous storage or lytic vacuoles, whereas decreased expression has an opposite effect. In addition, endocytic/vacuolar trafficking of the well-established vacuolar cargo PIN2 is affected, suggesting that both trafficking to the vacuole and vacuolar function and/or morphology depend on SAC2–SAC5 function.

Although direct biochemical evidence is lacking, the close similarity of SAC2–SAC5 to both SAC1 and Fig4p, which have in vitro phosphatase activity on PtdIns(3,5)P_2 (15, 16, 25), the modified lipid levels in the lines with engineered *SAC2–SAC5* expression, and the abundance of PtdIns3P in the tonoplast imply that SAC2–SAC5 are involved in the PtdIns(3,5)P_2-to-PtdIns3P conversion. The combined observations establish the presence and important function of PPI metabolites in the plant tonoplast.

Materials and Methods

A full discussion of materials and methods can be found in *SI Materials and Methods*.

Plant Material and Growth Conditions. Seeds of *A. thaliana* L. Heynh (accession Columbia-0) were stratified for 2 d in the dark at 4 °C and germinated vertically in Petri dishes containing 0.8% agar and 0.5× Murashige and Skoog (1/2MS) medium (Duchefa) with 1% sucrose at 18 °C in a 16-h light/8-h dark photoperiod. For analysis of arrested seedlings, we used 1/2MS medium with 0.8% agar without sucrose and liquid 1/2MS medium for all chemical treatments. The mutants *sac1* (Salk_031386), *sac2* (GABI_599E04), *sac3* (Salk_023548), *sac4* (Salk_056500), and *sac5* (Salk_125856) were identified from available T-DNA collections (51) and obtained from the Arabidopsis Biological Resource Center collection (GenBank accession numbers AAP49834.1, AAP49835.1, AAP49836.1, AAP49837.1, and AAP49838.1, respectively).

Construct Preparation and Transformation. To generate the *35S::SAC-GFP* and *35S::SAC-RFP* transgenic lines, we amplified the corresponding genomic sequences without a STOP codon. For details, see *SI Materials and Methods*.

Genotyping and Quantitative RT-PCR. T-DNA insertional lines were genotyped with the left border primers LBb1.3 and LB-08474 for the SALK and GABI-Kat lines in combination with the gene-specific primers (Table S1). For details, see *SI Materials and Methods*.

Drug and Lipid Treatments. Five-day-old seedlings were incubated with the following chemicals: 8 μM FM4-64 (Invitrogen) for 3 h, 2 μM LysoTracker Red (Invitrogen) for 50 min, 33 μM wortmannin (Sigma-Aldrich) for 3 h, and 50 μM BFA (Sigma-Aldrich) for 90 min. Vacuoles were visualized with FM4-64 as described (35). For the PI treatments, see *SI Materials and Methods*.

Phenotypic Analysis. Root length, hypocotyl length, and lateral root density were measured by the Java-based ImageJ application (http://rsb.info.nih.gov/ij). At least 20 seedlings were measured in three independent experiments giving the same statistically significant results. The statistical significance was evaluated with the Student *t* test.

Extraction and Quantification of Lipids. Lipids were extracted from 2-wk-old plants grown on 1/2MS medium under a long-day regime (16-h light/8-h dark) and analyzed as described (44) with slight modifications. For details, see *SI Materials and Methods*.

Protein Immunolocalization. Immunolocalizations on 6-d-old seedlings were done as described in detail in *SI Materials and Methods*.

TEM on Roots. Root tips of 4-d-old seedlings of double *sac3 sac4* and triple *sac3 sac4 sac5* mutants were excised and processed as described (33).

ACKNOWLEDGMENTS. We thank Peter Marhavý for technical assistance. This work was supported by grants from the Research Foundation-Flanders (Odysseus), the Körber-Stiftung, and the European Research Council (Project ERC-2011-StG-20101109-PSDP). E.F. is indebted to the European Molecular Biology Organization for a postdoctoral fellowship (LTF 795-2012).

1. Di Paolo G, De Camilli P (2006) Phosphoinositides in cell regulation and membrane dynamics. *Nature* 443(7112):651–657.
2. Thole JM, Nielsen E (2008) Phosphoinositides in plants: Novel functions in membrane trafficking. *Curr Opin Plant Biol* 11(6):620–631.
3. Thole JM, Vermeer JEM, Zhang Y, Gadella TWJ, Jr., Nielsen E (2008) *Root hair defective4* encodes a phosphatidylinositol-4-phosphate phosphatase required for proper root hair development in *Arabidopsis thaliana*. *Plant Cell* 20(2):381–395.
4. Ischebeck T, Seiler S, Heilmann I (2010) At the poles across kingdoms: Phosphoinositides and polar tip growth. *Protoplasma* 240(1-4):13–31.
5. Munnik T, Nielsen E (2011) Green light for polyphosphoinositide signals in plants. *Curr Opin Plant Biol* 14(5):489–497.
6. van Leeuwen W, Okrész L, Bögre L, Munnik T (2004) Learning the lipid language of plant signalling. *Trends Plant Sci* 9(8):378–384.
7. Hsu F, Mao Y (2013) The Sac domain-containing phosphoinositide phosphatases: Structure, function, and disease. *Front Biol* 8(4):395–407.
8. Gary JD, Wurmser AE, Bonangelino CJ, Weisman LS, Emr SD (1998) Fab1p is essential for PtdIns(3)P 5-kinase activity and the maintenance of vacuolar size and membrane homeostasis. *J Cell Biol* 143(1):65–79.
9. Odorizzi G, Babst M, Emr SD (1998) Fab1p PtdIns(3)P 5-kinase function essential for protein sorting in the multivesicular body. *Cell* 95(6):847–858.
10. Shaw JD, Hama H, Sohrabi F, DeWald DB, Wendland B (2003) PtdIns(3,5)P_2 is required for delivery of endocytic cargo into the multivesicular body. *Traffic* 4(7):479–490.
11. Takasuga S, Sasaki T (2013) Phosphatidylinositol-3,5-bisphosphate: Metabolism and physiological functions. *J Biochem* 154(3):211–218.
12. Rudge SA, Anderson DM, Emr SD (2004) Vacuole size control: Regulation of PtdIns(3,5)P_2 levels by the vacuole-associated Vac14-Fig4 complex, a PtdIns(3,5)P_2-specific phosphatase. *Mol Biol Cell* 15(1):24–36.
13. Botelho RJ, Efe JA, Teis D, Emr SD (2008) Assembly of a Fab1 phosphoinositide kinase signaling complex requires the Fig4 phosphoinositide phosphatase. *Mol Biol Cell* 19(10):4273–4286.
14. Jin N, et al. (2008) VAC14 nucleates a protein complex essential for the acute interconversion of PI3P and PI(3,5)P(2) in yeast and mouse. *EMBO J* 27(24):3221–3234.
15. Duex JE, Nau JJ, Kauffman EJ, Weisman LS (2006) Phosphoinositide 5-phosphatase Fig 4p is required for both acute rise and subsequent fall in stress-induced phosphatidylinositol 3,5-bisphosphate levels. *Eukaryot Cell* 5(4):723–731.
16. Meijer HJG, Divecha N, van den Ende H, Musgrave A, Munnik T (1999) Hyperosmotic stress induces rapid synthesis of phosphatidyl-D-inositol 3,5-bisphosphate in plant cells. *Planta* 208:294–298.
17. Bavaro L, et al. (2007) Lipid content in higher plants under osmotic stress. *Bioelectrochemistry* 70(1):12–17.
18. Whitley P, Hinz S, Doughty J (2009) *Arabidopsis* FAB1/PIKfyve proteins are essential for development of viable pollen. *Plant Physiol* 151(4):1812–1822.
19. Bak G, et al. (2013) Rapid structural changes and acidification of guard cell vacuoles during stomatal closure require phosphatidylinositol 3,5-bisphosphate. *Plant Cell* 25(6):2202–2216.
20. Vermeer JEM, et al. (2006) Visualization of PtdIns3P dynamics in living plant cells. *Plant J* 47(5):687–700.
21. Hughes WE, Cooke FT, Parker PJ (2000) Sac phosphatase domain proteins. *Biochem J* 350(Pt 2):337–352.
22. Williams ME, et al. (2005) Mutations in the *Arabidopsis* phosphoinositide phosphatase gene *SAC9* lead to overaccumulation of PtdIns(4,5)P_2 and constitutive expression of the stress-response pathway. *Plant Physiol* 138(2):686–700.
23. Gong P, Wu G, Ort DR (2006) Slow dark deactivation of *Arabidopsis* chloroplast ATP synthase caused by a mutation in a nonplastidic SAC domain protein. *Photosynth Res* 88(2):133–142.
24. Vollmer AH, Youssef NN, DeWald DB (2011) Unique cell wall abnormalities in the putative phosphoinositide phosphatase mutant *AtSAC9*. *Planta* 234(5):993–1005.
25. Zhong R, et al. (2005) Mutation of SAC1, an *Arabidopsis* SAC domain phosphoinositide phosphatase, causes alterations in cell morphogenesis, cell wall synthesis, and actin organization. *Plant Cell* 17(5):1449–1466.
26. Zhong R, Ye Z-H (2003) The SAC domain-containing protein gene family in *Arabidopsis*. *Plant Physiol* 132(2):544–555.
27. Stolz LE, Huynh CV, Thorner J, York JD (1998) Identification and characterization of an essential family of inositol polyphosphate 5-phosphatases (*INP51*, *INP52* and *INP53* gene products) in the yeast *Saccharomyces cerevisiae*. *Genetics* 148(4):1715–1729.
28. Guo S, Stolz LE, Lemrow SM, York JD (1999) *SAC1*-like domains of yeast *SAC1*, *INP52*, and *INP53* and of human synaptojanin encode polyphosphoinositide phosphatases. *J Biol Chem* 274(19):12990–12995.
29. Uemura T, et al. (2010) Vacuolar/pre-vacuolar compartment Qa-SNAREs VAM3/SYP22 and PEP12/SYP21 have interchangeable functions in *Arabidopsis*. *Plant J* 64(5):864–873.
30. Vida TA, Emr SD (1995) A new vital stain for visualizing vacuolar membrane dynamics and endocytosis in yeast. *J Cell Biol* 128(5):779–792.
31. Ueda T, Yamaguchi M, Uchimiya H, Nakano A (2001) Ara6, a plant-unique novel type Rab GTPase, functions in the endocytic pathway of *Arabidopsis thaliana*. *EMBO J* 20(17):4730–4741.
32. Laxmi A, Pan J, Morsy M, Chen R (2008) Light plays an essential role in intracellular distribution of auxin efflux carrier PIN2 in *Arabidopsis thaliana*. *PLoS ONE* 3(1):e1510.
33. Feraru E, et al. (2010) The AP-3 β adaptin mediates the biogenesis and function of lytic vacuoles in *Arabidopsis*. *Plant Cell* 22(8):2812–2824.
34. Kato T, et al. (2002) SGR2, a phospholipase-like protein, and ZIG/SGR4, a SNARE, are involved in the shoot gravitropism of *Arabidopsis*. *Plant Cell* 14(1):33–46.
35. Kleine-Vehn J, et al. (2008) Differential degradation of PIN2 auxin efflux carrier by retromer-dependent vacuolar targeting. *Proc Natl Acad Sci USA* 105(46):17812–17817.
36. Zwiewka M, et al. (2011) The AP-3 adaptor complex is required for vacuolar function in *Arabidopsis*. *Cell Res* 21(12):1711–1722.
37. Tse YC, et al. (2004) Identification of multivesicular bodies as prevacuolar compartments in *Nicotiana tabacum* BY-2 cells. *Plant Cell* 16(3):672–693.
38. Wang J, Cai Y, Miao Y, Lam SK, Jiang L (2009) Wortmannin induces homotypic fusion of plant prevacuolar compartments. *J Exp Bot* 60(11):3075–3083.
39. Geldner N, Friml J, Stierhof Y-D, Jürgens G, Palme K (2001) Auxin transport inhibitors block PIN1 cycling and vesicle trafficking. *Nature* 413(6854):425–428.
40. Robert S, et al. (2010) ABP1 mediates auxin inhibition of clathrin-dependent endocytosis in *Arabidopsis*. *Cell* 143(1):111–121.
41. Petrásek J, et al. (2006) PIN proteins perform a rate-limiting function in cellular auxin efflux. *Science* 312(5775):914–918.
42. Abas L, et al. (2006) Intracellular trafficking and proteolysis of the *Arabidopsis* auxin-efflux facilitator PIN2 are involved in root gravitropism. *Nat Cell Biol* 8(3):249–256.
43. Baster P, et al. (2013) SCF(TIR1/AFB)-auxin signalling regulates PIN vacuolar trafficking and auxin fluxes during root gravitropism. *EMBO J* 32(2):260–274.
44. König S, Hoffmann M, Mosblech A, Heilmann I (2008) Determination of content and fatty acid composition of unlabeled phosphoinositide species by thin-layer chromatography and gas chromatography. *Anal Biochem* 378(2):197–201.
45. Ischebeck T, et al. (December 10, 2013) Phosphatidylinositol 4,5-bisphosphate influences PIN polarization by controlling clathrin-mediated membrane trafficking in *Arabidopsis*. *Plant Cell*, 10.1105/tpc.113.116582.
46. Simon MLA, et al. (October 21, 2013) A multi-colour/multi-affinity marker set to visualize phosphoinositide dynamics in *Arabidopsis*. *Plant J*, 10.1111/tpj.12358.
47. Ikonomov OC, Sbrissa D, Shisheva A (2001) Mammalian cell morphology and endocytic membrane homeostasis require enzymatically active phosphoinositide 5-kinase PIKfyve. *J Biol Chem* 276(28):26141–26147.
48. Gary JD, et al. (2002) Regulation of Fab1 phosphatidylinositol 3-phosphate 5-kinase pathway by Vac7 protein and Fig4, a polyphosphoinositide phosphatase family member. *Mol Biol Cell* 13(4):1238–1251.
49. Gao X-Q, Zhang XS (2012) Metabolism and roles of phosphatidylinositol 3-phosphate in pollen development and pollen tube growth in *Arabidopsis*. *Plant Signal Behav* 7(2):165–169.
50. Hirano T, Matsuzawa T, Takegawa K, Sato MH (2011) Loss-of-function and gain-of-function mutations in *FAB1A/B* impair endomembrane homeostasis, conferring pleiotropic developmental abnormalities in *Arabidopsis*. *Plant Physiol* 155(2):797–807.
51. Alonso JM, et al. (2003) Genome-wide insertional mutagenesis of *Arabidopsis thaliana*. *Science* 301(5633):653–657.